Fermi National Accelerator Laboratory

FERMILAB-Pub-97/045-E
E687

Analysis of the D^+, $D_s^+ \to \pi^-\pi^+\pi^+$ Dalitz Plots

P.L. Frabetti et al.
The E687 Collaboration

Fermi National Accelerator Laboratory
P.O. Box 500, Batavia, Illinois 60510

February 1997

Submitted to *Physics Letters B*

Operated by Universities Research Association Inc. under Contract No. DE-AC02-76CH03000 with the United States Department of Energy

Analysis of the D^+, $D_s^+ \to \pi^-\pi^+\pi^+$ Dalitz Plots.

E687 Collaboration

P. L. Frabetti

Dip. di Fisica dell'Università and INFN - Bologna, I-40126 Bologna, Italy

H. W. K. Cheung [a], J. P. Cumalat, C. Dallapiccola [b], J. F. Ginkel, W. E. Johns [c], M. S. Nehring [d], E. W. Vaandering

University of Colorado, Boulder, CO 80309, USA

J. N. Butler, S. Cihangir, I. Gaines, P. H. Garbincius, L. Garren, S. A. Gourlay, D. J. Harding, P. Kasper, A. Kreymer, P. Lebrun, S. Shukla, M. Vittone

Fermilab, Batavia, IL 60510, USA

S. Bianco, F. L. Fabbri, S. Sarwar, A. Zallo

Laboratori Nazionali di Frascati dell'INFN, I-00044 Frascati, Italy

C. Cawlfield, R. Culbertson [e], R. W. Gardner [f], R. Greene [g], A. Rahimi, J. Wiss

University of Illinois at Urbana-Champaign, Urbana, IL 61801, USA

G. Alimonti, G. Bellini, M. Boschini, D. Brambilla, B. Caccianiga, L. Cinquini [h], M. Di Corato, P. Dini, M. Giammarchi, P. Inzani, F. Leveraro, S. Malvezzi, D. Menasce, E. Meroni, L. Milazzo, L. Moroni, D. Pedrini, L. Perasso, F. Prelz, A. Sala, S. Sala, D. Torretta

Dip. di Fisica dell'Università and INFN - Milano, I-20133 Milan, Italy

D. Buchholz, D. Claes [i], B. Gobbi, B. O'Reilly [h]

Northwestern University, Evanston, IL 60208, USA

J. M. Bishop, N. M. Cason, C. J. Kennedy [j], G. N. Kim [k], T. F. Lin, D. L. Puseljic [j], R. C. Ruchti, W. D. Shephard, J. A. Swiatek [l], Z. Y. Wu [m]

University of Notre Dame, Notre Dame, IN 46556, USA

V. Arena, G. Boca, G. Bonomi, C. Castoldi, G. Gianini, M. Merlo, S. P. Ratti, C. Riccardi, L. Viola, P. Vitulo

Dip. di Fisica Nucleare e Teorica dell'Università and INFN - Pavia, I-27100 Pavia, Italy

A. Lopez, L. Mendez, E. Montiel, D. Olaya, E. Ramirez, C. Rivera, Y. Zhang

University of Puerto Rico at Mayaguez, Puerto Rico

G. P. Grim, J.M. Link, V. S. Paolone [n], P. M. Yager

University of California-Davis, Davis, CA 95616, USA

J. R. Wilson

University of South Carolina, Columbia, SC 29208, USA

J. Cao, M. Hosack, J. Hughes, P. D. Sheldon

Vanderbilt University, Nashville, TN 37235, USA

F. Davenport

University of North Carolina-Asheville, Asheville, NC 28804, USA

K. Danyo [o], T. Handler

University of Tennessee, Knoxville, TN 37996, USA

B. G. Cheon [p], Y.S. Chung, J. S. Kang, K. Y. Kim, K.B. Lee, S.S. Myung

Korea University, Seoul 136-701, Korea

Abstract

An amplitude analysis of the $D^+, D_s^+ \to \pi^-\pi^+\pi^+$ Dalitz plots is presented using data collected by the Fermilab high-energy photoproduction experiment E687. The data are fitted to a model consisting of a sum of relativistic Breit-Wigner amplitudes for the intermediate two-body resonant decay modes plus a flat *non-resonant* contribution. From the fit we derive decay fractions and relative phases. We also present measurements of $\frac{\Gamma(D^+\to\pi^-\pi^+\pi^+)}{\Gamma(D^+\to K^-\pi^+\pi^+)}$ and $\frac{\Gamma(D_s^+\to\pi^-\pi^+\pi^+)}{\Gamma(D_s^+\to K^-K^+\pi^+)}$.

I. INTRODUCTION

Recently, amplitude analysis of non-leptonic decays has emerged as an excellent tool for studying charm-hadron dynamics. In particular, the amplitude analysis of D^+ and D_s^+ decays into three pions addresses some crucial issues in the phenomenology of charm decay. The D_s^+ decay into three pions is, in fact, the best candidate to proceed through an annihilation diagram, since annihilation of the two initial quarks is Cabibbo favoured and not suppressed as in the D^+ decay.

In this letter we present an amplitude analysis of the D^+ and $D_s^+ \to \pi^-\pi^+\pi^+$ final states*, where the contributing decay channels are allowed to interfere coherently. The measurement of the branching ratios $\frac{\Gamma(D^+\to\pi^-\pi^+\pi^+)}{\Gamma(D^+\to K^-\pi^+\pi^+)}$ and $\frac{\Gamma(D_s^+\to\pi^-\pi^+\pi^+)}{\Gamma(D_s^+\to K^-K^+\pi^+)}$ is also presented. These measurements are based on the data collected during the 1990-91 run of the Fermilab photoproduction experiment E687.

The E687 detector was designed and used to study the interaction of high-energy ($\simeq$ 200 GeV) photons on a Beryllium target. The detector is a large-aperture, fixed-target, multiparticle magnetic spectrometer with excellent Čerenkov particle identification and vertexing capabilities. Secondary charm vertices were isolated using a 12-plane microstrip system. A more complete description of the detector appears in Ref. [1].

II. CANDIDATE SELECTION

Two complementary approaches were used to reconstruct the primary (charm-production) and secondary (charm-decay) vertices in our sample. These were called the "candidate-driven" vertex method and the "stand-alone" vertex method; a detailed discussion of the two methods can be found in Refs. [1,2]. The results we quote in the present paper are based on the former method owing to its higher efficiency. The second method has been used to evaluate the consistency of the results and any possible systematic effects introduced by the vertexing algorithm.

We begin by describing the selection of the "candidate-driven" D^+, $D_s^+ \to \pi^-\pi^+\pi^+$ candidates. For each event, all combinations of three pions, each having longitudinal

---

*Throught this paper the charge conjugate state is always implied.

momentum greater than 4 GeV/c[†] and a Čerenkov signature inconsistent with electron, kaon, kaon/proton and proton, were tried out; only those combinations forming a common (secondary) vertex with a confidence level exceeding 1% were retained. The primary vertex candidate was required to be formed by at least two other tracks in addition to the seed track (defined by the three-momentum of the D candidate passing through the reconstructed secondary vertex) and was required to lie in the fiducial volume of the Be target. The secondary vertex was required to be downstream of the primary vertex by at least 5 standard deviations ($\ell > 5\sigma_\ell$)[‡].

To ensure the secondary vertex was well isolated, leftover tracks not found in the primary vertex were required to be inconsistent with emerging from the secondary vertex, and secondary tracks were required not to point towards the primary vertex. The further requirement that the secondary vertex lie outside the target (a requirement which we will call the "air-gap cut") significantly reduces the non-charm background as shown by Fig. 1. The air-gap cut increases the signal-to-background ratio by about a factor of four for both D^+ and D_s^+. Backgrounds from the decay $D^{*+} \to D^0(\to K^-\pi^+)\pi^+$, with the kaon wrongly identified as a pion, and the much rarer decay $D^{*+} \to D^0(\to \pi^-\pi^+)\pi^+$ were eliminated by the additional requirement that the $M_{K\pi\pi} - M_{K\pi}$ and $M_{\pi\pi\pi} - M_{\pi\pi}$ mass differences lie outside the D^{*+} signal regions. The signal region has a reconstructed mass within 2σ of the signal peak centroid found in the fit.

The much cleaner sample of Fig. 1b was used to perform the Dalitz-plot analysis of the three-pion decay. The mass plot was fitted using two Gaussians for the D^+ and D_s^+ signals, a Gaussian shape for the $K\pi\pi$ reflection tail at high masses and a second-order polynomial for the remaining background. We obtain 235.6 ± 20.1 and 97.9 ± 12.2 events for the D^+ and D_s^+ yields respectively. The corresponding mass plot, as obtained by the "stand-alone" vertexing method with the requirement that the secondary vertex lie outside the target, is shown in Fig. 2. For this sample the D^+ and D_s^+ yields turn out to be 187.3 ± 19.4 and 63.3 ± 12.2 respectively.

The fitted yields and the signal/background ratios for the full sample, the air-gap cut sample (used for the present analysis) and the stand-alone method sample are listed

---

[†]This cut eliminates the background at low momenta while retaining almost 93% of the signal.

[‡]The variable ℓ is the signed 3-dimensional separation between vertices and σ_ℓ is the error on ℓ computed on an event-by-event basis, including effects of multiple Coulomb scattering.

in Table I.

Table I: Invariant mass spectrum fit results.

$D^+ \to \pi^-\pi^+\pi^+$	Yield	Signal/Background
Sample type		
Full sample	633.5 ± 54.0	0.61 ± 0.08
Air-gap cut	235.6 ± 20.1	7.47 ± 1.00
Stand alone method	187.3 ± 19.4	5.07 ± 1.32
$D_s^+ \to \pi^-\pi^+\pi^+$		
Full sample	433.8 ± 53.6	0.38 ± 0.06
Air-gap cut	97.9 ± 12.2	4.22 ± 0.85
Stand alone method	63.3 ± 12.2	2.08 ± 0.06

III. THE DALITZ PLOTS AND THE FIT FORMALISM

The Dalitz plots for the D^+ and D_s^+ signal regions, defined as those within $\pm 2\sigma$ from the corresponding mass peaks, are shown in Figs. 3a and 3b respectively for the "candidate-driven" method, and in Figs. 3c and 3d for the "stand-alone" method. We have plotted the lower value of the two possible $m^2(\pi^+\pi^-)$ combinations on the abscissa and the higher value on the ordinate.

We performed a continuous maximum likelihood fit to the two Dalitz plots to measure the fraction of decays into the intermediate modes as well as their relative phases. Following our previous works [2], the total amplitude is assumed to consist of a flat, uniform term for the three-body non-resonant contribution plus a sum of functions B which represent intermediate strong resonances and decay angular-momentum conservation. The fit parameters are the amplitude coefficients a_i and phases δ_i*:

$$\mathcal{A}(D) = a_0 e^{i\delta_0} + \sum_i a_i e^{i\delta_i} B(abc|r) \tag{1}$$

Explicitly, a, b and c label the final-state particles, $B(abc|r) = BW(a,b|r)\mathcal{S}(a,c)$ where $BW(a,b|r)$ is the Breit-Wigner function:

*We fix the parameters of the dominant decay mode to have amplitude coefficient $a_i = 1$ and phase $\delta_i = 0$.

$$BW(a,b|r) = \frac{F_D F_r}{M_r^2 - M_{ab}^2 - i\Gamma M_r} \tag{2}$$

and $\mathcal{S}(a,c) = 1$ for a spin-0 resonance, $\mathcal{S}(a,c) = (-2\vec{c}\cdot\vec{a})$ for a spin-1 resonance and $\mathcal{S}(a,c) = 2(|\vec{c}||\vec{a}|)^2(3\cos^2\theta^* - 1)$ for a spin-2 resonance. The $\vec{c}$ and $\vec{a}$ are the three-momenta of particles c and a measured in the ab rest frame, and $\cos\theta^* = \vec{c}\cdot\vec{a}/|\vec{c}||\vec{a}|$. The momentum-dependent form factors F_D and F_r represent the strong coupling at each decay vertex. For each resonance of mass M_r and spin j, we use a width [3]:

$$\Gamma = \Gamma_0 \left[\frac{\vec{p}}{\vec{p_0}}\right]^{2j+1} \frac{M_0}{M_{ab}} \frac{F_r^2(p)}{F_r^2(p_0)}, \tag{3}$$

where $\vec{p}$ is the decay three-momentum in the resonance rest frame and the subscript 0 denotes the on-shell values.

The order of particle labels is important in defining our phases (e.g., for vector decays, exchanging a and b results in a phase shift of 180 degrees). The $\pi^+\pi^-$ amplitudes were Bose-symmetrized by computing $B(\pi^-\pi_1^+\pi_2^+|(\pi^+\pi^-)) + B(\pi^-\pi_2^+\pi_1^+|(\pi^+\pi^-))$. The resulting probability density function was properly weighted by a function to correct for geometrical acceptance and reconstruction efficiency. Monte Carlo studies confirmed the biases caused by finite-mass resolution to be negligible.

All the resonances decaying into $\pi^+\pi^-$ with a sizeable branching fraction have been considered as possible intermediate states with special treatment for the following two cases.

To retain consistency within our formalism, we employed a slightly modified version of the parametrization described by the WA76 Collaboration [4] for the $f_0(980)$ amplitude, which is written

$$BW(a,b|r) = \frac{F_D F_r}{M_r^2 - M_{ab}^2 - i(\Gamma_\pi + \Gamma_K)M_r} \tag{4}$$

with

$$\Gamma_\pi = g_\pi \left[\frac{M_{KK}^2}{4} - M_\pi^2\right]^2, \Gamma_K = \frac{g_K}{2}\left[\left(\frac{M_{K^-K^+}^2}{4} - M_{K^+}^2\right)^{1/2} + \left(\frac{M_{K^-K^+}^2}{4} - M_{K^0}^2\right)^{1/2}\right]$$

The coupling constants were set to the WA76 values, $g_\pi = 0.28 \pm 0.04$ and $g_K = 0.56 \pm 0.18$. We found that the exact parametrization of the $f_0(980)$ amplitude had negligible effects on the fitted decay fractions of the landmark resonances.

The parameters describing the S-wave dipion resonances have recently been called into question[†]; in the next section we will discuss how we deal with this problem.

The shape of the background contribution was parametrized from polynomial fits to the Dalitz plot of the left mass sideband, extending from -7σ to -3σ, for the D^+ analysis and of the right mass sideband, from 3σ to 7σ, for the D_s analysis[‡].

The number of background events expected in the signal region was determined from the polynomial shape of the background as returned from the fit of the $\pi^-\pi^+\pi^+$ invariant mass distribution; the signal to background ratio [§] is quoted for both D^+ and D_s^+ in Table I. The uncertainties in both the background shape parameters and normalization were taken into account in our fit procedure; all background parameters were included as additional fit parameters, but were tied to the results of the sideband fits through the inclusion in the likelihood of a χ^2 term, constructed using the covariance matrix of the sideband fits.

We fitted the D^+ and D_s^+ samples separately by forming likelihood functions $\mathcal{L}$ consisting of signal and background probability densities. We then minimized the function $-2\ln\mathcal{L}$ over the signal parameters, a_i and δ_i. The decay fraction into a given mode was computed by integrating the signal intensity for that mode alone divided by the integrated intensity with all modes present[*]. The fact that these fractions do not sum to unity reflects the presence of interference between the modes.

Checks of the fitting procedure were made using Monte Carlo techniques and all

---

[†]The PDG94 [5] collected all the $\pi\pi$ elastic S-wave resonances measured in the 1000-1500 MeV$/c^2$ mass region under one entry only, the $f_0(1300)$, with no clear indication of the mass and the width. The recent PDG96 [6], instead, lists several scalar states, in the same mass region, which could decay in $\pi\pi$, namely the $f_0(400-1200)$, $f_0(1370)$ and $f_0(1500)$; the masses and the widths of the first two states are only estimates, which span a wide range of values, while the branching ratio of $f_0(1500)$ in $\pi^+\pi^-$ is not even quoted.

[‡]For the D^+ analysis, the large $K\pi\pi$ contamination in the low-mass sideband was removed by requiring the candidate mass to be incompatible with the $D^+ \to K\pi\pi$ hypothesis.

[§]This ratio was computed including all the events within 2σ of the fitted gaussian centroid.

[*]This definition, which has become conventional, allows direct comparison of fit results independently of the amplitude formalism choice.

biases were found to be small compared to the statistical errors.

The systematic errors in the decay fractions and phases reflect uncertainties in reconstruction efficiency and background parametrization. For example, since our reconstruction and trigger efficiency is a strong function of the D momentum, we compared the results from separate fits to the Dalitz plot for candidates both above and below the observed mean D momentum. In a similar way, we split our data into two separate samples depending on the Čerenkov identification of the opposite-sign pion of the combination: in the first sample we put all the candidates having a strict Čerenkov requirement (the opposite-sign pion identified as pion definite or pion/electron ambiguous) and in the other the remaining candidates with a looser requirement. Decay fractions and phases were also recomputed separately for the data collected in the first run period (1990) and for those collected during the second period (1991). A first contribution to the systematic error was evaluated from the consistency of these split samples using the *S-factor method* of the Particle Data Group [6] and taking into account the full covariance matrix of each independent result.

The assumption that the shape of the background in the Dalitz plot is well represented by that of the chosen sidebands could lead to an additional contribution to the systematic error. To investigate this possibility, we drastically varied the background parametrization from a second-order polynomial (in the D_s case) or fourth-order (in the D^+ case) to a constant term. Similarly, we varied the efficiency function parametrizations by changing the order of the polynomials employed in the fit. The observed variation on the results has been added in quadrature to the systematic errors.

We did not observe any significant variation between results based on the "candidate-driven" and "stand alone" samples; the two sets of results were consistent with a common mean at a confidence level of 96% in the D^+ case and of 59% in the D_s^+ case. Systematic uncertainty due to the statistical errors reported for the $\pi^+\pi^-$ resonance parameters, with the exception of the highly uncertain scalar resonances in the 1000-1500 MeV/c^2 mass region, were found to be negligibly small and are not quoted in the tables as separate errors.

IV. RESULTS FOR THE $D_S^+ \to \pi^-\pi^+\pi^+$ FINAL STATE

The $D_s^+ \to \pi^-\pi^+\pi^+$ Dalitz plot shown in Fig. 3b shows several clear features. The $f_0(980)$ band, previously observed by E691 * [7], is evident around the $\pi^+\pi^-$ mass-squared value of 1 $(GeV/c^2)^2$. There is an accumulation of events near the sharp corner on the right side of the Dalitz plot, which could be attributed to the third helicity lobe of the $f_2(1270)$ (Fig. 4 shows the expected shape of this resonance on the Dalitz plot, along with its two mass-squared projections). The non-resonant contribution should be presumably small because of the absence of population in the upper corner of the Dalitz plot. By way of contrast, there appears to be a uniform band around 2 $(\mathrm{GeV}/c^2)^2$, whose structure suggests the presence of a scalar resonance in the $\pi^+\pi^-$ mass around 1.5 GeV/c^2. Given the major uncertainty about dipion scalar resonances in this mass region†, we decided to use our own data to find the parameters for a single state which best reproduces the Dalitz plot. We performed several fits of our D_s^+ Dalitz plot by varying the mass (1200 MeV - 1600MeV) and the width (25 MeV - 400 MeV) of this state, which was parametrized as a Breit-Wigner resonance. Fits were performed taking into account all the possible additional contributions from a non-resonant component and the well established resonances, $f_0(980)$, $f_2(1270)$ and $\rho(770)$. Fig. 5a and 5b show the likelihood behaviour around the minimum as a function of the resonance parameters. A clear minimum in $-2\ln\mathcal{L}$ was found at $M = 1.475\,GeV/c^2$ and $\Gamma = 100\,MeV/c^2$. These two values have been used to quote our measurements and the two corresponding $\pm1\sigma$ ranges to assess the related systematics‡. The parameters of this state, which we denote as $\mathcal{S}(1475)$, are remarkably consistent with the $f_0(1500)$ entry of PDG96§.

---

*There are two main differences between our analysis and that performed by E691. The E691 formalism does not allow for interference among different amplitudes and does not account for additional resonances which are considered in the present analysis. This prevents us from a meaningful comparison of our Dalitz plot results with those of E691.

†See footnote on page 6.

‡We also tried potential 1^- and 2^+ states in this region, but their best likelihood values were significantly worst than the scalar.

§Although the mass and width of this state are in excellent agreement with the $f_0(1500)$ entry in PDG96 [6], we note that several interfering resonances in this region could equally

The features previously described are confirmed by the complete five amplitude fit results of the Dalitz plot, which are listed in Table II:

Table II: Fit results for $D_s^+ \to \pi^-\pi^+\pi^+$

Decay mode	Decay fraction	Phase (degrees)	Amplitude Coefficient
NR	$0.121 \pm 0.115 \pm 0.044$	$235 \pm 22 \pm 2$	0.34 ± 0.14
$\rho(770)\pi$	$0.023 \pm 0.027 \pm 0.011$	$53 \pm 44 \pm 10$	0.15 ± 0.09
$f_2(1270)\pi$	$0.123 \pm 0.056 \pm 0.018$	$100 \pm 18 \pm 6$	0.34 ± 0.09
$f_0(980)\pi$	$1.074 \pm 0.140 \pm 0.043$	$0(fixed)$	$1(fixed)$
$\mathcal{S}(1475)\pi$	$0.274 \pm 0.114 \pm 0.019$	$234 \pm 15 \pm 4$	0.50 ± 0.13
$-2\ln\mathcal{L} = 125.1$			

It appears, from this table, that only the $f_2(1270)$, $f_0(980)$ and $\mathcal{S}(1475)$ resonances have non-zero amplitude coefficients exceeding 3 sigma significance. As a final gauge of the systematics we present in Table III the result of a fit with only these resonances included.

Table III: Results for D_s^+ removing minor amplitudes from the fit

Decay mode	Decay fraction	Phase (degrees)	Amplitude Coefficient
$f_2(1270)\pi$	0.147 ± 0.053	83 ± 16	0.42 ± 0.08
$f_0(980)\pi$	0.848 ± 0.067	$0(fixed)$	$1.0(fixed)$
$\mathcal{S}(1475)\pi$	0.341 ± 0.078	210 ± 10	0.63 ± 0.09
$-2\ln\mathcal{L} = 133.2$			

The results of the two fits are shown in Fig. 6.

Evidence for a non-resonant decay, as well as for a $\rho(770)\pi^+$ contribution, would have important theoretical implications. While the latter decay is expected to be heavily suppressed, evidence for the NR channel could be attributed to a weak annihilation process or to final state interactions [8]. To this extent, we evaluated the upper limits

---

well describe the D_s^+ Dalitz plot. For this reason we will hedge our bets by refering to this amplitude contribution as the $\mathcal{S}(1475)$ throughout this paper.

for these two decay fractions, which turn out to be $< 26.9\%$ at 90% CL for the NR component and $< 7.3\%$ at 90% CL for the $\rho(770)\pi^+$.

However, we warn the reader that, in contrast with the $\rho(770)\pi^+$ case, assessing the presence of the non-resonant component in a decay is a very difficult task, which would require at least a high statistical sample since a coherent sum of wide resonances could easily mimic an almost flat contribution. Even more, it turns out that, in our case, it is enough to introduce a narrow scalar such as $\mathcal{S}(1475)$ to trigger this effect, which is demonstrated by the anticorrelation between the NR and $\mathcal{S}(1475)$ coefficients, as returned by fits to several Monte Carlo simulations of the experiment assuming as input our final fit result (see Fig. 7); events, which cannot be attributed to the $f_0(980)\pi^+$, $f_2(1270)\pi^+$ or $\rho(770)\pi^+$, are easily absorbed by either the $\mathcal{S}(1475)\pi^+$ or the non-resonant components.

V. RESULTS FOR THE $D^+ \to \pi^-\pi^+\pi^+$ FINAL STATE

The D^+ decay into three pions, in contrast with the D_s^+ decay, which seems to be mostly a two body process, exhibits, just by visual inspection, a much more uniform population across the Dalitz surface. The only feature which is clearly evident is the peak around 0.6 $(GeV/c^2)^2$, indicative of the presence of $\rho(770)\pi^+$.

Fig. $8a, b$ and c show a mass projection comparison between our fit result and the data including all our final set of contributions, NR, $\rho(770)\pi^+$, $f_2(1270)\pi^+$ and $f_0(980)\pi^+$, while Fig. $8d, e$ and f show this same comparison when only the NR and $\rho(770)\pi^+$ contributions are included. The resulting decay fractions of the four amplitude fit are listed in Table IV, together with the corresponding phases.

Table IV: Fit results for $D^+ \to \pi^-\pi^+\pi^+$

Decay mode	Decay fraction	Phase (degrees)	Amplitude coefficient
NR	$0.589 \pm 0.105 \pm 0.081$	$0(fixed)$	$1(fixed)$
$\rho(770)\pi$	$0.289 \pm 0.055 \pm 0.058$	$27 \pm 14 \pm 11$	0.70 ± 0.11
$f_2(1270)\pi$	$0.052 \pm 0.034 \pm 0.035$	$207 \pm 17 \pm 4$	0.30 ± 0.11
$f_0(980)\pi$	$0.027 \pm 0.031 \pm 0.038$	$197 \pm 28 \pm 24$	0.22 ± 0.13
$-2\ln\mathcal{L} = 385.4$			

As a final gauge of the systematics, in analogy with what we did for D_s^+, we show the parameters of the two amplitude fit in Table V.

Table V: Results for D^+ removing minor amplitudes from the fit

Decay mode	Decay fraction	Phase (degrees)	Amplitude coefficient
NR	0.768 ± 0.046	$0(fixed)$	$1.0(fixed)$
$\rho(770)\pi$	0.232 ± 0.046	36 ± 9	0.55 ± 0.07
$-2\ln\mathcal{L} = 400.8$			

VI. THE BRANCHING RATIO MEASUREMENTS

The same data, as selected for the Dalitz analysis, were used to measure the following branching ratios: $\frac{\Gamma(D^+\to\pi^-\pi^+\pi^+)}{\Gamma(D^+\to K^-\pi^+\pi^+)}$ and $\frac{\Gamma(D_s^+\to\pi^-\pi^+\pi^+)}{\Gamma(D_s^+\to K^-K^+\pi^+)}$.

Whenever possible, the cuts employed for the normalization modes were the same as those used for the three-pion Dalitz analysis, with the exception of the longitudinal momentum cut, which was applied only to the three-pion final states. The $K\pi\pi$ and $KK\pi$ final states were selected by requiring for the kaons a Čerenkov signature consistent with kaon definite, kaon/pion ambiguous or kaon-proton ambiguous. To remove the significant contamination of the $D_s^+ \to K^-K^+\pi^+$ signal due to the misidentification of a pion in $D^+ \to K^-\pi^+\pi^+$ decays, we employed an "anti-reflection" cut, which rejected candidates when the reconstructed $K^-\pi^+\pi^+$ mass was inside 2σ of the D^+ peak.

The final mass plots used for the branching ratio measurements are shown in Fig. 1b and in Fig. 9a, b. The signal peaks were fitted to Gaussian shapes, while background was fitted to a second-order polynomial. The shape of the $K\pi\pi$ reflection peak, in the $\pi\pi\pi$ final state, was parametrized from MonteCarlo and was not allowed to vary in the final fit to the data. The final results for the branching ratios are quoted in Table VI together with the other available measurements.

From the $\frac{\Gamma(D_s^+\to\pi^-\pi^+\pi^+)}{\Gamma(D_s^+\to K^-K^+\pi^+)}$ measurement, using the PDG96 [6] value for $\Gamma(\phi \to K^+K^-)$ together with our previous result [2] on $\frac{\Gamma(D_s^+\to\phi\pi^+)}{\Gamma(D_s^+\to K^-K^+\pi^+)}$, we can derive the $\frac{\Gamma(D_s^+\to\pi^-\pi^+\pi^+)}{\Gamma(D_s^+\to\phi\pi^+)}$ branching ratio, which is also quoted in Table VI.

Our results are in reasonable agreement with the previous determinations of the relative branching ratios and significantly increase the precision of the measurement.

The final measurements were checked by varying each of the vertex cuts individually; the results were always well within the errors.

Table VI: Branching-ratio measurement results

	$\frac{\Gamma(D^+\to\pi^-\pi^+\pi^+)}{\Gamma(D^+\to K^-\pi^+\pi^+)}$	$\frac{\Gamma(D_s^+\to\pi^-\pi^+\pi^+)}{\Gamma(D_s^+\to K^-K^+\pi^+)}$	$\frac{\Gamma(D_s^+\to\pi^-\pi^+\pi^+)}{\Gamma(D_s^+\to\phi\pi^+)}$.
E687	$0.043 \pm 0.003 \pm 0.003$	$0.265 \pm 0.041 \pm 0.031$	$0.328 \pm 0.058 \pm 0.058$
E691 [7]	$0.035 \pm 0.007 \pm 0.003$	–	$0.44 \pm 0.10 \pm 0.04$
WA82 [9]	$0.032 \pm 0.011 \pm 0.003$	–	$0.33 \pm 0.10 \pm 0.04$
MarkIII [10]	$0.042 \pm 0.016 \pm 0.010$	–	–

In analogy with what was done for the Dalitz analysis, estimates of the systematics were obtained by splitting our data into disjoint samples depending on the D^+ and D_s^+ momenta, the different periods in which the data were collected and the Čerenkov signature of the opposite-sign particle. For these measurements, we employed a slightly modified version of the *S-factor method* of the Particle Data Group [6], as illustrated in Ref. [11]. In particular, the *S-factor method* was used to separate true systematic variations from statistical fluctuations. The branching ratio was evaluated for each of the statistically independent subsamples and a *scaled variance* was calculated; the *split-sample* variance is defined as the difference between the reported statistical variance and the scaled variance when the scaled variance exceeds the statistical variance.

The additional systematic effects related to the different fit procedures were evaluated for the whole sample. The branching ratios were calculated varying the fit conditions* and the sample variance was used since the fit variants are all equally likely *a priori*.

VII. CONCLUSIONS

We have performed a fully coherent analysis of the resonant substructure of the D^+ and D_s^+ decays into three pions. The results show that, while the D^+ decay appears to be dominated by non-resonant and $\rho(770)\pi^+$ channels, the D_s^+ decay seems to proceed mainly through $f_0(980)\pi^+$ with smaller but significant contributions from a state which we are calling $\mathcal{S}(1475)$ and the $f_2(1270)$ resonance. The parameters of the $\mathcal{S}(1475)$

*These include the choice of the estimator, the background shape and the Gaussian parameters.

are completely consistent with the $f_0(1500)$ listing in the PDG96 [6] but we cannot rule out possible contributions from several resonances in this general mass region. In the D_s^+ case, no evidence for the $\rho(770)\pi^+$ was found and the evidence for the non-resonant component is very weak. The same data have been used to measure the relative branching ratios of these decays into three pions with respect to the best measured D^+ and D_s^+ decays.

VIII. ACKNOWLEDGEMENTS

We wish to acknowledge the assistance of the staffs of the Fermi National Accelerator Laboratory, the INFN of Italy, and the physics departments of the collaborating institutions. We also wish to acknowledge useful discussions with Prof. P. Ratcliffe of Milan University, Prof. L. Maiani of the Rome University and Prof. I. Bigi of Notre Dame University. This research was supported in part by the National Science Foundation, the U.S. Department of Energy, the Italian Istituto Nazionale di Fisica Nucleare and Ministero dell'Università e della Ricerca Scientifica e Tecnologica, and the Korean Science and Engineering Foundation.

REFERENCES

[a] Present address: Fermilab, Batavia, IL 60510, USA.

[b] Present address: University of Maryland, College Park, MD 20742, USA.

[c] Present address: University of South Carolina, Columbia, SC 29208, USA.

[d] Present address: Vanderbilt University, Nashville, TN 37235, USA.

[e] Present address: Enrico Fermi Institute, University of Chicago, Chicago, IL 60637, USA.

[f] Present address: Department of Physics, Indiana University, Bloomington, Indiana, IN 47405, USA.

[g] Present address: Syracuse University, Syracuse, NY 13244-1130, USA.

[h] Present address: University of Colorado, Boulder, CO 80309, USA.

[i] Present address: University of New York, Stony Brook, NY 11794, USA.

[j] Present address: AT&T, West Long Branch, NJ 07765, USA.

[k] Present address: Pohang Accelerator Laboratory, Pohang, Korea.

[l] Present address: Science Applications International Corporation, McLean, VA 22102, USA.

[m] Present address: Gamma Products Inc., Palos Hills, IL 60465, USA.

[n] Present address: Department of Physics and Astronomy, University of Pittsburgh, 3941 O'Hara St., Pittsburgh, PA 15260, USA.

[o] Present address: Brookhaven National Laboratory, Upton, NY 11793-5000, USA.

[p] Present address: KEK, National Laboratory for High Energy Physics, Tsukuba 305, Japan.

[1] E687 Collab., P.L. Frabetti *et al.*, Nucl. Instrum. Methods. A 320 (1992) 519;
E687 Collab., P.L. Frabetti *et al.*, Nucl. Instrum. Methods. A 329 (1993) 62.

[2] E687 Collab., P.L. Frabetti *et al.*, Phys. Lett. B 331 (1994) 217;
E687 Collab., P.L. Frabetti *et al.*, Phys. Lett. B 351 (1995) 591.

[3] ARGUS Collab., H. Albrecht et al., Phys. Lett. B308, (1993) 435.

[4] WA76 Collab., T.A. Armstrong et al., Z. Phys. C51 (1991) 351.

[5] PDG94, L.Montanet *et al.*, Phys. Rev. D50 (1994) 1173. (Review of Particle Properties)

[6] PDG96, R.M.Barnett *et al.*, Phys. Rev. D54 (1996) 1. (Review of Particle Properties)

[7] E691 Collab., J.C. Anjos *et al.*, Phys. Rev. Lett. 62 (1989) 125.

[8] I.I.Bigi, Proceedings of the CCAST Symposium, Vol. 2 "Charm Physics", Ming-Han and Tao Huang (eds.), Gordon and Breach Science Publishers, (1987) 339.
T.E.Browder, K.Honscheid, D.Pedrini, Ann. Rev. Nucl. Part. Sci. 46 (1996) 395.

[9] WA82 Collab., M.Adamovich et al., Phys. Lett. B 305 (1993) 177.

[10] Mark III Collab., R.M.Baltrusaitis et al., Phys. Rev. Lett. 55 (1985) 150.

[11] E687 Collab., P.L. Frabetti *et al.*, Phys. Lett. B 354 (1995) 486.

IX. FIGURES

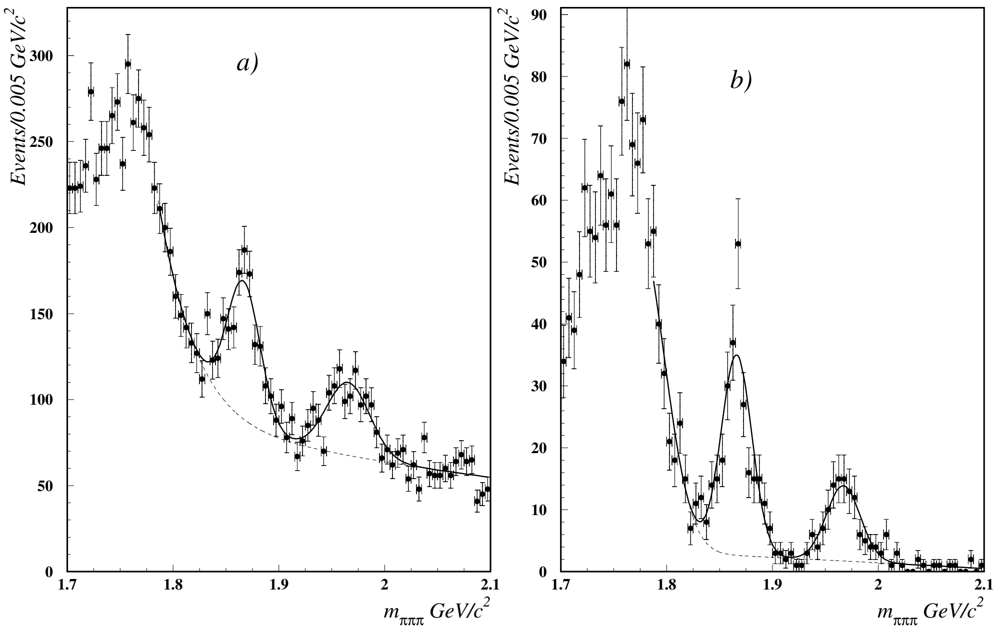

Fig. 1: 3π mass combinations:
a) full sample, b) requiring the secondary vertex out of target.

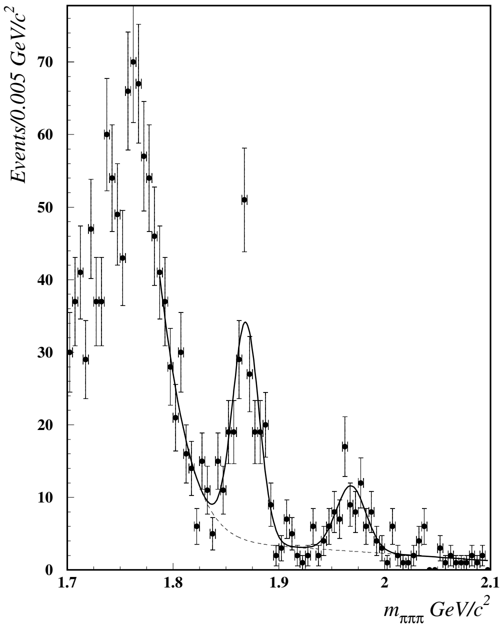

Fig. 2: 3π mass combinations from the "*stand alone*" method, requiring the secondary vertex out of target.

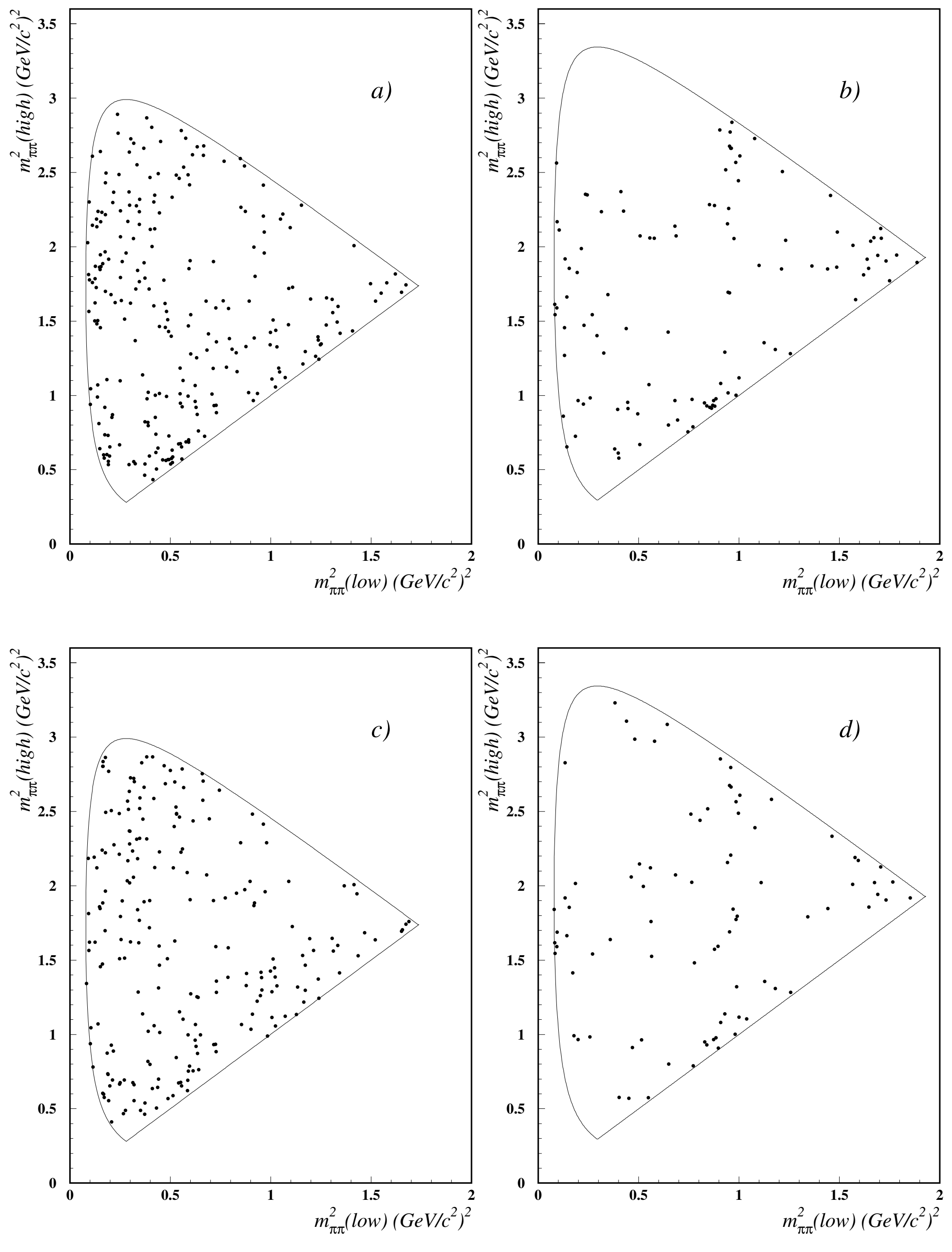

Fig. 3 D^+ and $D_s^+ \to \pi^-\pi^+\pi^+$ Dalitz plots:

a) and b) are for the D^+ and D_s^+ signal regions respectively.

c) and d) are the corresponding plots as obtained by the "*stand alone*" method.

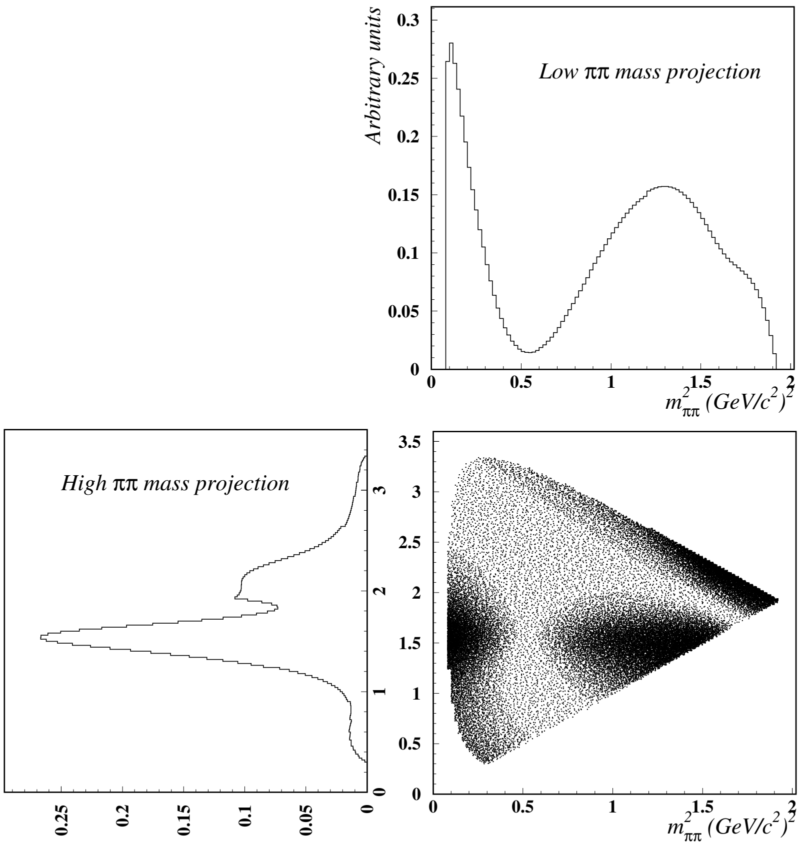

Fig. 4: Dalitz plot of the expected $D_s^+ \to f_2(1270)\pi^+$ shape along with its two mass-squared projections

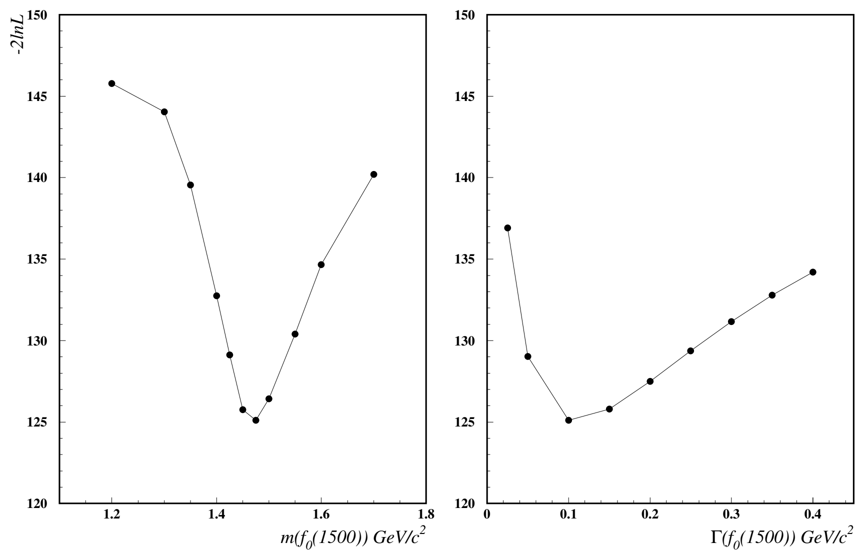

Fig. 5 The -2ln $\mathcal{L}$ values of the fit for $D_s^+ \to \pi^-\pi^+\pi^+$ obtained by varying the mass and the width of a Breit-Wigner scalar resonance: the minimum was found at $M = 1.475$ GeV/c^2 and $\Gamma = 0.1$ GeV/c^2. The likelihood behaviour along the mass and the width axes, around the minimum, is shown in Fig. 5a and 5b respectively.

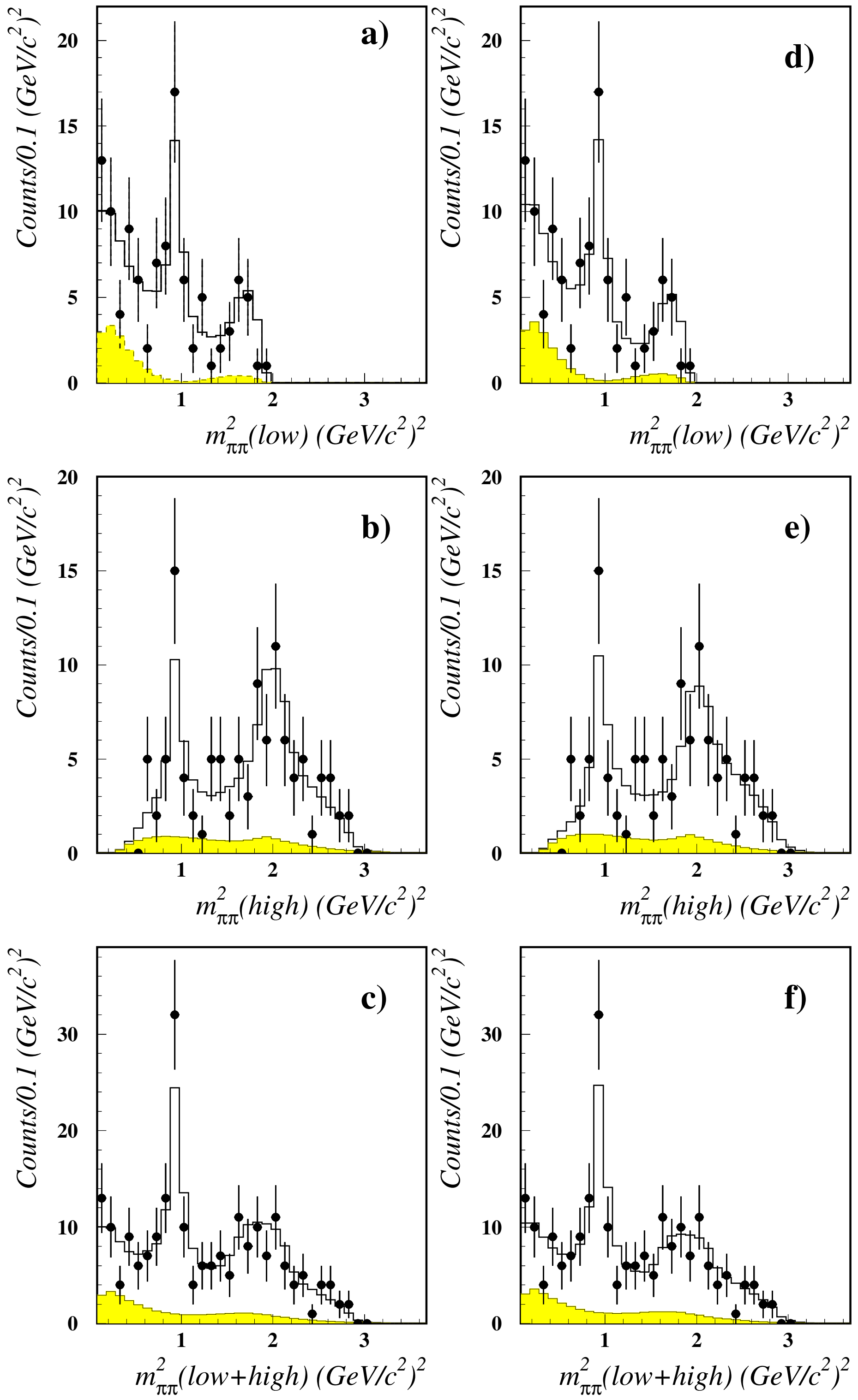

Fig. 6: The Dalitz projections and fit results for $D_s^+ \to \pi^-\pi^+\pi^+$: five amplitude fit (**a**, **b**, **c**) and reduced three amplitude fit (**d** **e**, **f**). The continuous line represents the fit result and the shaded area the background contribution.

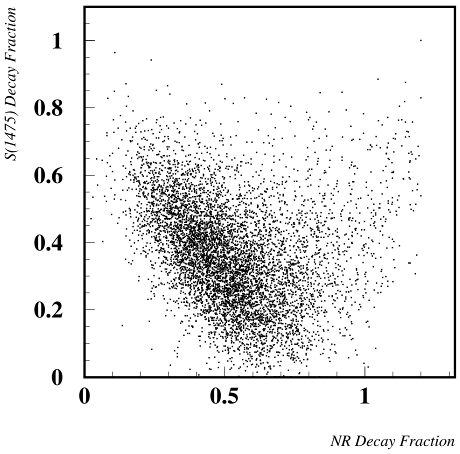

Fig. 7: Correlation between NR and $\mathcal{S}(1475)$ from a $D_s^+ \to \pi^-\pi^+\pi^+$ Monte Carlo simulation.

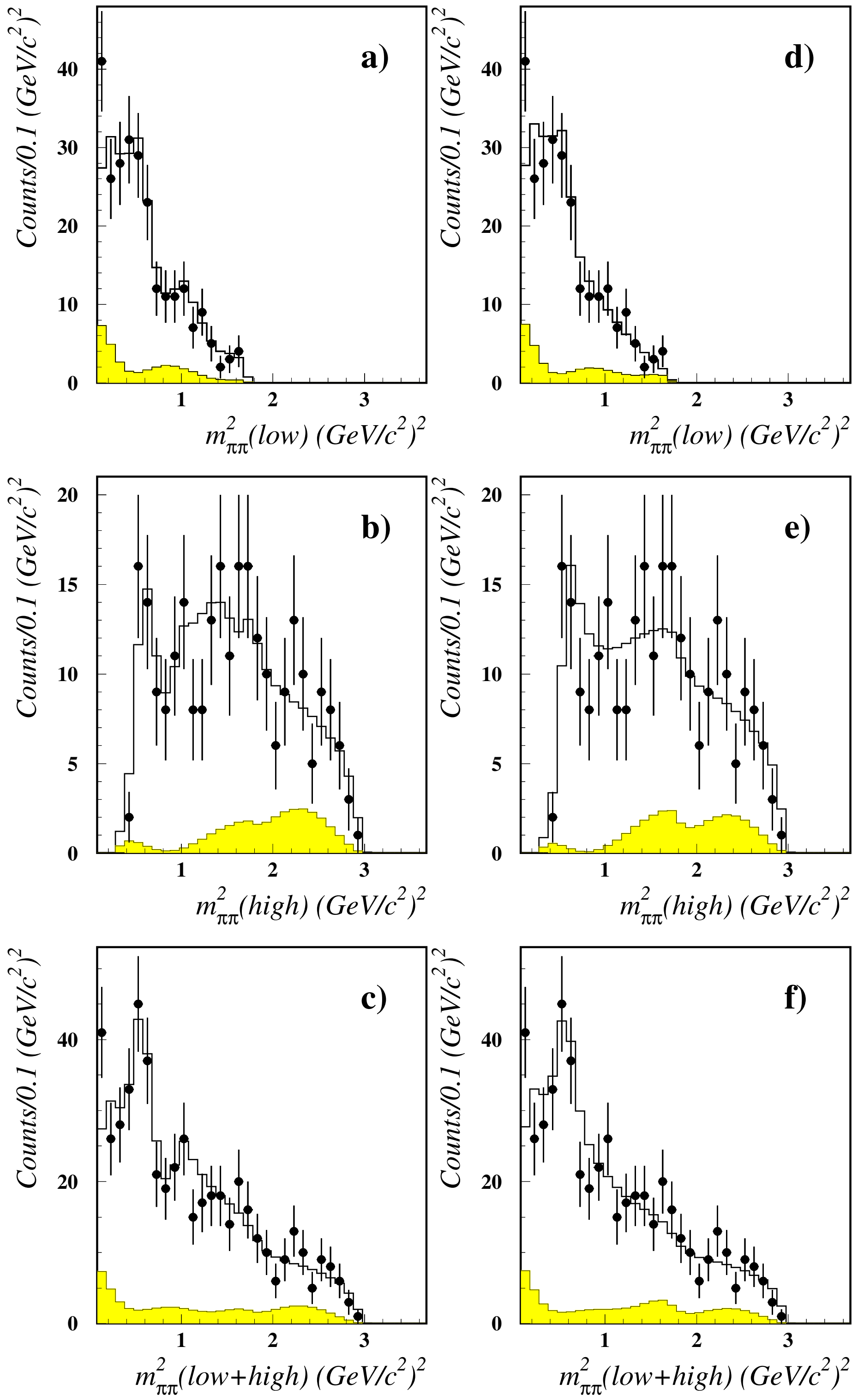

Fig. 8: The Dalitz projections and fit results for $D^+ \to \pi^-\pi^+\pi^+$: four amplitude fit (**a**, **b**, **c**) and reduced two amplitude fit (**d** **e**, **f**).

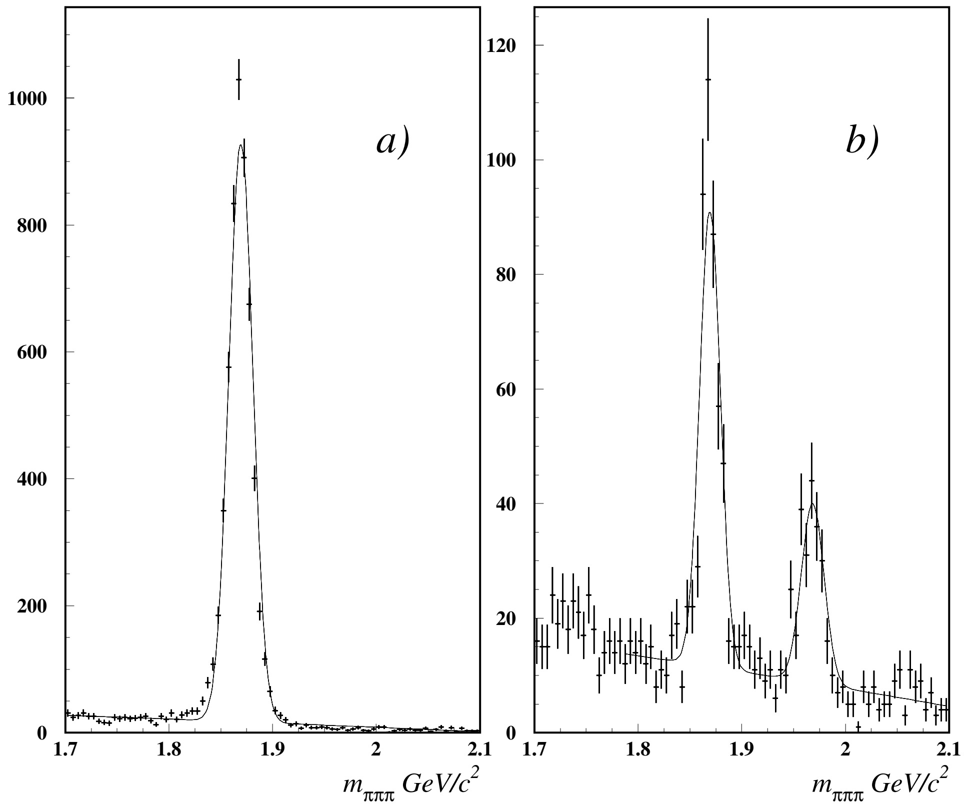

Fig. 9: a) $K^-\pi^+\pi^+$ and b) $K^-K^+\pi^+$ mass spectra for the normalization channels in the branching ratio measurement.